

TESS: Text-to-Text Self-Conditioned Simplex Diffusion

Rabeeh Karimi Mahabadi^{1,4} Jaesung Tae² Hamish Ivison³
 James Henderson⁴ Iz Beltagy³ Matthew E. Peters^{3*} Arman Cohan^{2,3*}

¹EPFL ²Yale University ³Allen Institute for AI ⁴Idiap Research Institute

rabeeh.karimimahabadi@epfl.ch, {jake.tae, arman.cohan}@yale.edu
 {hamishi, beltagy, matthewp}@allenai.org, james.henderson@idiap.ch

Abstract

Diffusion models have emerged as a powerful paradigm for generation, obtaining strong performance in various domains with continuous-valued inputs. Despite the promises of fully non-autoregressive text generation, applying diffusion models to natural language remains challenging due to its discrete nature. In this work, we propose Text-to-text Self-conditioned Simplex Diffusion (TESS), a text diffusion model that is fully non-autoregressive, employs a new form of self-conditioning, and applies the diffusion process on the logit simplex space rather than the typical learned embedding space. Through extensive experiments on natural language understanding and generation tasks including summarization, text simplification, paraphrase generation, and question generation, we demonstrate that TESS outperforms state-of-the-art non-autoregressive models and is competitive with pretrained autoregressive sequence-to-sequence models.

1 Introduction

Diffusion models (Sohl-Dickstein et al., 2015; Ho et al., 2020; Song et al., 2021) have achieved state-of-the-art performance in various continuous-valued domains, such as image (Nichol and Dhariwal, 2021), audio (Kong et al., 2020; Shen et al., 2023), video (Ho et al., 2022), and text-conditional image generation (Saharia et al., 2022; Ramesh et al., 2022). However, due to the inherently discrete nature of text, applying diffusion models to natural language remains a challenging task.

Inspired by the success of diffusion for continuous domains, recent works have adapted diffusion to discrete spaces, such as text (Austin et al., 2021; Hoogeboom et al., 2021; Savinov et al., 2021; Reid et al., 2022). One line of work proposes diffusing the model latent space by adding Gaussian noise

to input word embeddings (Li et al., 2022b). Another approach, SSD-LM (Han et al., 2022), adds noise to the vocabulary probability simplex. Direct diffusion on the probability simplex is desirable (Richemond et al., 2022) as it eliminates the need for an extra step to map diffused embeddings to actual discrete inputs or auxiliary methods such as binary encoding (Chen et al., 2022). Despite its strong performance, however, SSD-LM has several shortcomings. Notably, it is semi-autoregressive and restricted to generating text in blocks of 25 tokens, which hinders the potential benefits of full diffusion, e.g., the ability to perform arbitrary infilling, flexible generation, and a global view of the sequence. It also does not include self-conditioning (Chen et al., 2022), which has been shown to improve model performance (Strudel et al., 2022). Moreover, SSD-LM lacks extensive comparisons against other embedding-based diffusion baselines for natural language tasks.

In this work, we present TESS, a diffusion-based model for natural language tasks, which overcomes several limitations of prior works: restrictions on scale (Hoogeboom et al., 2021; Austin et al., 2021), dependence on pretrained embeddings (Strudel et al., 2022), semi-autoregressive nature (Han et al., 2022), and short generation length (Gong et al., 2022). TESS closely follows Han et al. (2022) by performing diffusion on the vocabulary logit space rather than the typical embedding space. Unlike SSD-LM, however, TESS is fully non-autoregressive and performs diffusion on the entire sequence. It also incorporates a novel form of self-conditioning, which empirically demonstrates competitive edge over the original self-conditioning method (Chen et al., 2022).

We evaluate TESS on a suite of natural language generation (NLG) tasks including summarization, text simplification, paraphrase generation, and question generation. Our empirical results surpass the current state-of-the-art non-autoregressive

* Equal advising.

and diffusion-based approaches and are on par with a strong pretrained encoder-decoder language model (Lewis et al., 2020). In particular, our proposed simplex-based self-conditioning method substantially improves generation quality. We also evaluate TESS on natural language understanding (NLU) tasks from the GLUE benchmark (Wang et al., 2019) and show that it performs comparably to strong masked language model baselines. Our contributions can be summarized as follows.

1. We demonstrate the effectiveness of a fully non-autoregressive scheme for text diffusion models, which outperforms existing parallel and autoregressive methods.
2. We propose a new self-conditioning method that exploits the simplex semantics of the diffusion space.
3. We evaluate our approach over a suite of diverse NLG and NLU tasks, highlighting the effectiveness of our text-to-text simplex diffusion paradigm.

We plan to release our trained models and code to promote open research in the field of diffusion-based text generation.

2 Background

We revisit continuous diffusion models (Sohl-Dickstein et al., 2015), following the formulation of Denoising Diffusion Models (Ho et al., 2020; Song et al., 2020).

Training Given a sample $\mathbf{x}_0 \in \mathbb{R}^d$ from a data distribution p_{data} , a forward diffusion process $q(\mathbf{x}_t | \mathbf{x}_{t-1})$ is a Markov chain that generates a sequence of latent variables $\mathbf{x}_1, \dots, \mathbf{x}_T$ by gradually adding Gaussian noise at each time step $t \in \{1, 2, \dots, T\}$ with variance $\beta_t \in \mathbb{R}_{>0}$:

$$q(\mathbf{x}_t | \mathbf{x}_{t-1}) = \mathcal{N}(\mathbf{x}_t; \sqrt{1 - \beta_t} \mathbf{x}_{t-1}, \beta_t \mathbf{I}). \quad (1)$$

Let $\epsilon_t \sim \mathcal{N}(0, \mathbf{I})$, $\alpha_t = 1 - \beta_t$, and $\bar{\alpha}_t = \prod_{s=1}^t \alpha_s$. Then sampling \mathbf{x}_t at an arbitrary time step t has the closed-form solution

$$\mathbf{x}_t = \sqrt{\bar{\alpha}_t} \mathbf{x}_0 + \sqrt{1 - \bar{\alpha}_t} \epsilon_t. \quad (2)$$

Given a well-behaved noise schedule $\{\beta_t\}_{t=1}^T$, \mathbf{x}_T follows a stationary prior distribution $\mathcal{N}(0, \mathbf{I})$. Therefore, if we can approximate the reverse process $q(\mathbf{x}_{t-1} | \mathbf{x}_t, \mathbf{x}_0)$ via a model $p_{\theta}(\mathbf{x}_{t-1} | \mathbf{x}_t)$ with parameters θ , then we can sample random noise

from a standard Gaussian and gradually denoise it to sample from p_{data} . The reverse process is thus parametrized as

$$p_{\theta}(\mathbf{x}_{t-1} | \mathbf{x}_t) = \mathcal{N}(\boldsymbol{\mu}_{\theta}(\mathbf{x}_t, t), \boldsymbol{\Sigma}_{\theta}(\mathbf{x}_t, t)). \quad (3)$$

The model is trained by minimizing the mean squared error between the ground-truth data \mathbf{x}_0 and its estimate $\hat{\mathbf{x}}_{\theta}$:¹

$$\mathcal{L} = \mathbb{E}_{t, q(\mathbf{x}_0), q(\mathbf{x}_t | \mathbf{x}_0)} \|\mathbf{x}_0 - \hat{\mathbf{x}}_{\theta}(\mathbf{x}_t, t)\|^2. \quad (4)$$

Noise Schedule The forward diffusion process is defined by a noise schedule. In this work, we follow the cosine schedule (Nichol and Dhariwal, 2021) for α_t :

$$\bar{\alpha}_t = \frac{f(t)}{f(0)}, \quad f(t) = \cos\left(\frac{t/T + s}{1+s} \cdot \frac{\pi}{2}\right)^2. \quad (5)$$

Inference In Song et al. (2020), model predictions are iteratively denoised for $t = T, \dots, 1$ starting from pure noise, following

$$\mathbf{x}_{t-1} = \sqrt{\alpha_{t-1}} \hat{\mathbf{x}}_{\theta} + \sqrt{1 - \alpha_{t-1}} \cdot \frac{\mathbf{x}_t - \sqrt{\alpha_t} \hat{\mathbf{x}}_{\theta}}{\sqrt{1 - \alpha_t}}.$$

We derive a simplified form of this inference procedure in Appendix B, which allows us to apply diffusion to text without employing auxiliary methods that map categorical data to continuous space, and vice versa (Richemond et al., 2022).

3 Method

In this section, we present TESS, a simplex diffusion-based text-to-text model. Building upon SSD-LM (Han et al., 2022), we propose a fully non-autoregressive model with self-conditioning.

Continuous Data Representation Let \mathcal{V} denote the vocabulary space. Following Han et al. (2022), we map the ID of each token to be generated $w \in \mathcal{V}$ to a k -logit simplex to produce $\mathbf{s}^w \in \{\pm k\}^{|\mathcal{V}|}$, whose i -th component satisfies

$$s_{(i)}^w = \begin{cases} k, & \text{if } i = w, \\ -k, & \text{otherwise,} \end{cases} \quad (6)$$

with a hyperparameter $k \in \mathbb{R}$. We then produce a probability simplex over \mathcal{V} via $\mathbf{p}^w = \text{softmax}(\mathbf{s}^w)$. Finally, we compute the weighted sum of word embeddings to obtain a continuous embedding vector, $\mathbf{h}^w = \mathbf{E} \mathbf{p}^w$, where $\mathbf{E} \in \mathbb{R}^{d \times |\mathcal{V}|}$ is the word embedding matrix, d denotes the size of the hidden dimension, and $\mathbf{h}^w \in \mathbb{R}^d$.

¹ Alternatively, we can train the model to predict the added noise; see Ho et al. (2020). See also Song et al. (2021) for a score-matching interpretation.

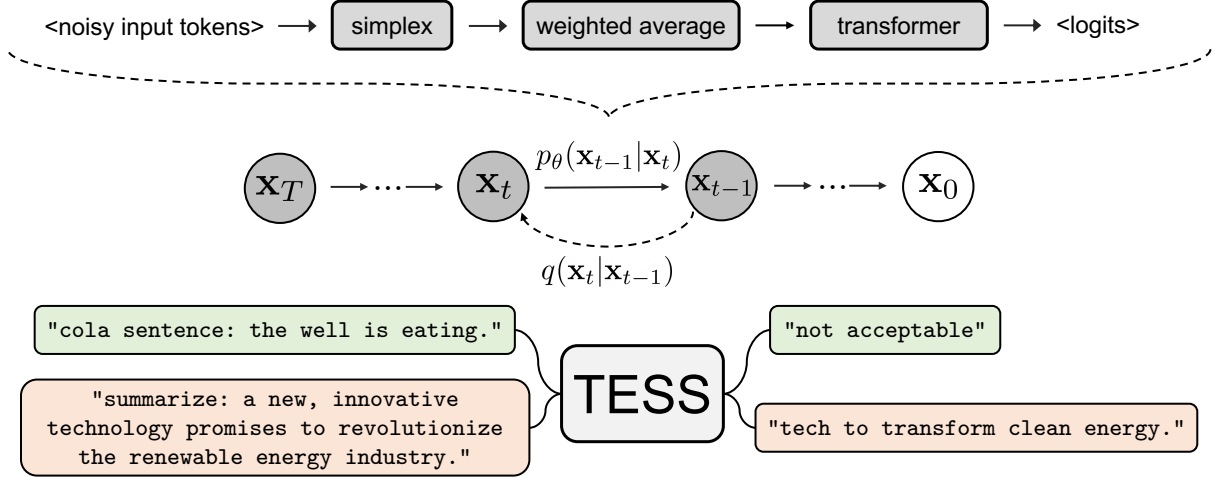


Figure 1: Overview of TESS. During training (top), we first add noise to the vocabulary probability simplex, compute a weighted average word embedding, and denoise it using a transformer encoder. To generate from our model, we begin with noise and iteratively refine it into a final logit distribution (middle). The resulting model can be used for a wide range of NLG and NLU end tasks (bottom).

Time Step Embeddings After computing the continuous word embeddings, we add the time step embeddings to inform the model of the current time step. Our time step embedding is a linear layer, and we feed scaled time steps t/T to this layer. The output is a time step embedding in \mathbb{R}^d that is added to \mathbf{h}_w to produce the final latent input vector.

Fully Non-Autoregressive Modeling Unlike SSD-LM, which feeds small blocks of text to semi-autoregressively generate sequences of text, we feed the entire latent vector into an encoder transformer model. This is a key difference between our approach and SSD-LM, as it allows for a fully non-autoregressive model capable of generating sequences of any length. In practice, our evaluation tasks often require output sequences of 100 tokens or more, and by moving to a fully non-autoregressive paradigm, we are able to generate entire output sequences in parallel without resorting to semi-autoregressive generation.

Forward Diffusion Let $\mathbf{w} = (w_1, \dots, w_L)$ be a sentence of L tokens such that $w_i \in \mathcal{V}$, and $\mathbf{S}_0 = (\mathbf{s}^{w_1}, \dots, \mathbf{s}^{w_L}) \in \{\pm k\}^{L \times |\mathcal{V}|}$ be the k -logit simplex representation of \mathbf{w} . We add noise to the k -logit simplex representation during training according to

$$\mathbf{S}_t = \sqrt{\bar{\alpha}_t} \mathbf{S}_0 + \sqrt{1 - \bar{\alpha}_t} \boldsymbol{\epsilon}_t, \quad (7)$$

where subscript denotes the time step and $\boldsymbol{\epsilon}_t \sim \mathcal{N}(0, k^2 \mathbf{I})$.

Training Typical diffusion models are trained with mean squared error loss as in Equation (4) to predict the ground-truth data. This objective is known to be unstable for text diffusion models (Dieleman et al., 2022). Strudel et al. (2022) froze word embeddings and used specific scaling to deal with training instability. In this work, following Han et al. (2022), we instead compute the usual cross-entropy loss between the ground-truth tokens \mathbf{w} and the model prediction given a noisy logit simplex \mathbf{S}_t at time step t .

$$\mathcal{L} = \mathbb{E}_{t, q(\mathbf{S}_0), q(\mathbf{S}_t | \mathbf{S}_0)} \left[- \sum_{i=1}^L \log p_{\theta}(w_i | \mathbf{S}_t, t) \right]. \quad (8)$$

Sampling During inference, we sample \mathbf{S}_T from the prior $\mathcal{N}(0, k^2 \mathbf{I})$ and run the reverse process for $t = T, \dots, 1$ on the noisy k -logit simplex. The reverse process can be approximated via

$$\mathbf{S}_{t-1} = \sqrt{\bar{\alpha}_{t-1}} \hat{\mathbf{S}}_{\theta}(\mathbf{S}_t, t) + \sqrt{1 - \bar{\alpha}_{t-1}} \boldsymbol{\epsilon}_t. \quad (9)$$

See Appendix B for details. This resembles the forward process in Equation (7), which allows for an intuitive interpretation: to reverse one step from t , we take the model prediction $\hat{\mathbf{S}}_{\theta}$ as the hypothetical ground-truth, then corrupt it by $(t-1)$ time steps. To construct the model prediction, we project the logits predicted by the underlying encoder model via argmax as a pseudo-inverse of Equation (6) to match the initial k -logit representation:

$$\hat{s}_{(i)}^w = \begin{cases} k, & \text{if } i = \text{argmax}(\mathbf{s}^w), \\ -k, & \text{otherwise.} \end{cases} \quad (10)$$

Self-Conditioning In typical diffusion models, the model predicts the original data \mathbf{x}_0 conditioned on its corrupted version, i.e., $\hat{\mathbf{x}}_0^t = \hat{\mathbf{x}}_\theta(\mathbf{x}_t, t)$, where $\hat{\mathbf{x}}_0^t$ denotes the estimate of \mathbf{x}_0 at time step t . In this setting, the model’s estimates at previous time steps are discarded. However, in self-conditioning (Chen et al., 2022), the model conditions its prediction on both \mathbf{x}_t and its previously generated output, i.e., $\hat{\mathbf{x}}_0^t = \hat{\mathbf{x}}_\theta(\mathbf{x}_t, \hat{\mathbf{x}}_0^{t+1}, t)$. To adapt the model for self-conditioning, we stochastically zero out the self-condition such that

$$\hat{\mathbf{x}}_0^t = \begin{cases} \hat{\mathbf{x}}_\theta(\mathbf{x}_t, \hat{\mathbf{x}}_0^{t+1}, t), & \text{with probability } \rho \\ \hat{\mathbf{x}}_\theta(\mathbf{x}_t, 0, t), & \text{otherwise,} \end{cases} \quad (11)$$

where the self-conditioning previous prediction is computed as $\hat{\mathbf{x}}_0^{t+1} = \hat{\mathbf{x}}_\theta(\mathbf{x}_{t+1}, 0, t+1)$, with gradients detached. We always use self-conditioning during sampling.

In practice, self-conditioning is implemented by concatenating \mathbf{x}_t and $\hat{\mathbf{x}}_0^{t+1}$ along the feature dimension and projecting them back to the original dimension with a linear layer (Chen et al., 2022). In contrast, we propose a new self-conditioning method that exploits the simplex nature of our diffusion space. Let $\mathbf{s}_t \in \mathbb{R}^{|\mathcal{V}|}$ be a noised k -logit simplex for an arbitrary token w .² Instead of concatenating the previous prediction with \mathbf{s}_t and re-projecting, we first compute the average of simplex probabilities as

$$\mathbf{p}_{\text{avg}}^w = \frac{1}{2} (\text{softmax}(\mathbf{s}_t) + \text{softmax}(\hat{\mathbf{s}}_0^{t+1})). \quad (12)$$

Note that $\mathbf{p}_{\text{avg}}^w$ is a well-defined categorical distribution over \mathcal{V} with non-negative components that sum to 1. We then compute a continuous embedding vector, $\mathbf{h}^w = \mathbf{E}\mathbf{p}_{\text{avg}}^w$. This is more efficient than the original self-conditioning method, which projects down the concatenated vectors. In Section §6.2, we also demonstrate the empirical effectiveness of this method over the original.

Variable Sequence Length One notable challenge in non-autoregressive generation is the assumption of fixed sequence lengths during inference. To overcome this issue, we follow prior work in embedding-space diffusion, which uses padding tokens (Li et al., 2022b). Specifically, during training, we always pad the variable-length output sequence to a fixed length using padding tokens.

²We write \mathbf{s}_t^w as \mathbf{s}_t for brevity.

These padding tokens are included when computing the cross-entropy loss so that TESS learns to generate them. During inference, we specify the maximum sequence length and run sampling as usual. Due to the variable number of padding tokens used during training, TESS flexibly generates a variable-length output sequence by appropriately adapting the number of padding tokens. We show in Section §6.1 that TESS is capable of producing variable-length outputs to match the underlying distribution of sequence lengths in the ground-truth data.

4 Experiments

This section details the experimental evaluation of our proposed method. Specifically, we compare TESS with the current state-of-the-art models for non-autoregressive text-to-text generation and pretrained encoder-decoder models of comparable size on several NLG and NLU datasets. Results show that TESS outperforms prior work in non-autoregressive generation and is comparable with autoregressive models of similar size.

4.1 Tasks and Datasets

Paraphrase Generation The goal of paraphrase generation is to rephrase a sentence by generating an output that maintains the semantics of the original sentence, but with different words or sentence structures. We use the Quota Question Pairs (QQP) dataset,³ which is composed of 147K positive pairs. The dataset includes labels for whether a pair of questions has the same meaning. The positive pairs are used for paraphrase evaluation.

Text Simplification The objective of this task is to simplify complex sentences while retaining their original meaning. We use the NEWSEA-AUTO dataset (Jiang et al., 2020), which is composed of 666K complex-simplified sentences.

Question Generation The objective of this task is to generate a question given an input context. We use the QUASAR-T dataset (Dhingra et al., 2017) processed by Yuan et al. (2022), resulting in 119K document-question pairs.

Summarization This task entails generating a shorter version of a document while preserving important information. We evaluate our method on

³<https://www.kaggle.com/c/quora-question-pairs>

the CNN-DailyMail dataset (Hermann et al., 2015), which comprises 300K articles and summaries.

Classification We consider a set of classification tasks in the widely used GLUE benchmark (Wang et al., 2019) covering a variety of tasks, including paraphrase detection (MRPC, QQP), sentiment classification (SST-2), natural language inference (MNLI⁴, RTE, QNLI), and linguistic acceptability (CoLA).⁵

4.2 Baselines

We compare TESS to several autoregressive baselines as well as state-of-the-art text diffusion models. For autoregressive methods, we specifically consider the following fine-tuned models: GPT-2 (Radford et al., 2019), as a standard autoregressive LM; BART (Lewis et al., 2020), a strong sequence-to-sequence pretrained model; and GPVAE-T5 (Du et al., 2022), a latent-structured variable model and an extension to T5 (Raffel et al., 2020) capable of high-quality generations. For text diffusion models, we compare TESS to the following sequence-to-sequence diffusion models: Diffuser (Reid et al., 2022), DiffuSeq (Gong et al., 2022), SeqDiffuSeq (Yuan et al., 2022), and SUND-DAE (Savinov et al., 2021). We also compare TESS with LevT (Gu et al., 2019), a widely used iterative non-autoregressive model. Finally, given its strong relationship to our work, we also consider SSD-LM (Han et al., 2022) initialized from the same pretrained RoBERTa model as TESS and trained from the official SSD-LM codebase.⁶

4.3 Evaluation

For summarization, we use the standard ROUGE metric (Lin, 2004), reporting ROUGE-1 (R1), ROUGE-2 (R2), and ROUGE-L (R-L) variants as done in prior text summarization work (Lewis et al., 2020). We quantify both generation quality and diversity. For quality, we report BLEU (Papineni et al., 2002), ROUGE-L (Lin, 2004) and BERTScore (Zhang et al., 2020) following Gong et al. (2022) and Yuan et al. (2022). For diversity, we report distant unigrams (D-1) and diverse 4-grams (D-4) (Deshpande et al., 2018). For text simplification, we use the standard SARI (Xu et al.,

⁴We report the accuracy on the matched validation set.

⁵Following Devlin et al. (2019); Raffel et al. (2020), as a common practice and due to the adversarial nature of WNLI with respect to the training set, we do not experiment with WNLI.

⁶<https://github.com/xhan77/ssd-lm>

2016), and following Gong et al. (2022) and Yuan et al. (2022), we also include BLEU, BERTScore, and ROUGE-L metrics.

4.4 Implementation

We start from the RoBERTa pretrained checkpoint (Liu et al., 2019) and finetune the model on downstream tasks using our proposed self-conditioned simplex diffusion method. We initialize from a pretrained model as we find it results in faster convergence and improved performance in our pilot studies. Given the effectiveness of the diffusion-based training scheme, we expect it to scale to general pretraining and leave this area for future work. We use Hugging Face Transformers (Wolf et al., 2020) for pretrained checkpoints, model implementation, as well as training and evaluation scripts; Datasets (Lhoest et al., 2021) for accessing datasets and running evaluations; and Diffusers⁷ as the base library for our diffusion model pipeline. Our experiments are performed on 8 NVIDIA A6000/A100 GPUs. The number of diffusion sampling steps at inference time is set to $T = 1000$ for generation and $T = 10$ for classification tasks. During training, $T = 5000$. We set the simplex scale to $k = 5$. Additional details are listed in Appendix A.

5 Results

5.1 Paraphrase Generation

As seen in Table 1, TESS significantly outperforms GPT-2 and other non-autoregressive and diffusion baselines in quality metrics (BLEU, BERT, and ROUGE) while achieving parity in diversity metrics (D-1/D-4). Moreover, TESS obtains competitive overall performance with BART. Note that BART uses a denoising pretraining objective, which is substantially conducive to sequence-to-sequence tasks (Lewis et al., 2020); we do not perform any additional pretraining beyond RoBERTa’s checkpoint, which was only pretrained on the general masked language modeling objective. We suspect that TESS could significantly benefit from additional diffusion pretraining, as discussed in Section §8.

5.2 Text Simplification

Results of the text simplification task on the NEWSEA-AUTO dataset are presented in Table 2. TESS outperforms all baselines typically by large

⁷<https://huggingface.co/docs/diffusers>

Model	PARAPHRASE GENERATION			
	BLEU	BERT	R-L	D-1/4
Autoregressive Models				
BART (Lewis et al., 2020)	30.4	85.7	61.4	98.8/61.0
GPT-2 _{base} [†] (Radford et al., 2019)	19.8	82.5	52.1	98.0/62.5
GPT-2 _{large} [†] (Radford et al., 2019)	20.6	83.6	54.2	98.2/50.2
GPVAE-T5 [†] (Du et al., 2022)	24.1	84.7	58.9	96.9/61.7
Non-Autoregressive Models				
LevT [†] (Gu et al., 2019)	22.7	83.4	57.9	97.9/33.3
Non-Autoregressive Diffusion Models				
DiffuSeq [†] (Gong et al., 2022)	24.1	83.7	58.8	98.1/ 86.4
SeqDiffuSeq [†] (Yuan et al., 2022)	24.3	—	58.8	—
SSD-LM (Han et al., 2022)	22.9	83.8	58.3	98.8/57.3
TESS (Ours)	30.2	85.7	62.2	98.5/61.1

Table 1: Results on Paraphrase Generation task. Baseline values marked with [†] are taken from Gong et al. (2022). Boldfaced results show the best across all non-autoregressive models; underlined results are the best across all models.

margins, including both autoregressive and non-autoregressive models.

5.3 Question Generation

As shown in Table 3, TESS outperforms other diffusion and non-autoregressive models in terms of both quality of generation (BLEU, BERTScore, ROUGE) and diversity (D-1/D-4). It also consistently outperforms other autoregressive baselines except for BART, whose performance is closely matched by TESS.

5.4 Summarization

As shown in Table 4, TESS achieves competitive results with BART while outperforming prior diffusion work, Diffuser (Reid et al., 2022), by 1.9 ROUGE-L points, and its bootstrapped variants by 0.8 ROUGE-L points. Note that additional bootstrapping is orthogonal to their method and can be applied to TESS as well.

5.5 Text Classification

In this experiment, we evaluate TESS on classification tasks and directly compare our diffusion-based finetuning method with standard finetuning methods for supervised learning. To perform a controlled experiment, we compare TESS with a similar-sized RoBERTa, which we use to initialize our model. Note that since TESS is text-to-text, it can naturally handle classification tasks by generating class labels. For STS-B, which is a regression problem, we recast it as a 21-class classification

Model	TEXT SIMPLIFICATION			
	SARI	BLEU	BERT	R-L
Autoregressive Models				
BART (Lewis et al., 2020)	49.9	41.4	81.7	58.1
GPT-2 _{base} [†] (Radford et al., 2019)	—	30.8	80.2	54.6
GPT-2 _{large} [†] (Radford et al., 2019)	—	26.9	78.8	51.1
GPVAE-T5 [†] (Du et al., 2022)	—	33.9	81.7	58.3
Non-Autoregressive Models				
LevT [†] (Gu et al., 2019)	—	20.5	72.5	44.0
Non-Autoregressive Diffusion Models				
DiffuSeq [†] (Gong et al., 2022)	—	36.2	81.3	58.5
SeqDiffuSeq [†] (Yuan et al., 2022)	—	37.1	—	59.7
SSD-LM (Han et al., 2022)	36.3	12.5	69.5	39.6
TESS (Ours)	54.3	41.5	82.1	59.4

Table 2: Text simplification results on NEWSELAUTO dataset. Baseline values marked with [†] are taken from Gong et al. (2022). Boldfaced results show the best results across all non-autoregressive models; underlined results are the best results across all models.

problem following Raffel et al. (2020). We observe that TESS matches or outperforms finetuned RoBERTa on several tasks, achieving roughly 2-point gains on MRPC and RTE.

6 Analysis

6.1 Variable Length Output

Many text-diffusion models cannot flexibly generate variable length outputs and degrade in performance when handling longer sequences. For instance, Han et al. (2022) semi-autoregressively generates sequences in blocks of 25 tokens. TESS can flexibly generate long and variable-length sequences in a fully non-autoregressive fashion. In Figure 2, we display the generation length of TESS and compare it with both gold-label lengths and prediction lengths from BART, the strongest summarization baseline, on the CNN-DM summarization dataset. TESS is capable of producing output of variable lengths that match the underlying distribution of sequence lengths in the gold data.

To evaluate generation quality based on output length, we first group the generations for the CNN-DM dataset based on their lengths. Then, we compute the average ROUGE score on each group and compare the scores with BART. Figure 3 shows the results. We observe that the performance of our method is consistent with the BART baseline for variable target lengths, with shorter generations marginally underperforming BART and longer output matching BART’s performance.

Model	QUESTION GENERATION			
	BLEU	BERT	R-L	D-1/4
Autoregressive Models				
BART (Lewis et al., 2020)	17.4	66.2	38.8	98.2/61.7
GPT _{base} [†] (Radford et al., 2019)	7.4	60.5	27.2	96.0/92.2
GPT _{large} [†] (Radford et al., 2019)	11.1	63.5	32.2	96.7/80.6
GPVAE-T5 [†] (Du et al., 2022)	12.5	63.1	33.9	93.8/72.8
Non-Autoregressive Models				
LevT [†] (Gu et al., 2019)	9.3	54.9	28.9	89.1/47.8
Non-Autoregressive Diffusion Models				
DiffuSeq [†] (Gong et al., 2022)	17.3	61.2	36.7	90.6/ 81.0
SeqDiffuSeq [†] (Yuan et al., 2022)	17.5	—	36.1	—
SSD-LM (Han et al., 2022)	14.1	62.8	38.5	94.5/56.9
TESS (Ours)	19.5	65.8	38.9	97.1/63.0

Table 3: Results on Question Generation task. Baseline values marked with [†] are taken from [Gong et al. \(2022\)](#). Boldfaced results show the best results across all non-autoregressive models; underlined results are the best results across all models.

Model	CNN-DM		
	R1	R2	R-L
Autoregressive Models			
BART (Lewis et al., 2020)	<u>42.9</u>	<u>20.1</u>	40.1
Transformer (Vaswani et al., 2017) [◦]	—	—	36.8
Non-Autoregressive Diffusion Models			
SUNDAE (Savinov et al., 2021) [◦]	—	—	37.0
Diffuser (Reid et al., 2022) [◦]	—	—	37.8
Diffuser+ AR bootstrap [◦]	—	—	38.4
Diffuser + source bootstrap [◦]	—	—	38.9
TESS (Ours)	42.3	19.4	39.7

Table 4: Results on CNN-DailyMail dataset. Baseline values marked with [◦] are taken from [Reid et al. \(2022\)](#).

6.2 Self-Conditioning

To examine the impact of self-conditioning, we compare our proposed method with the original strategy ([Chen et al., 2022](#)) in text simplification and paraphrase generation tasks. As shown in Table 6, adding self-conditioning consistently improves results, with our variant delivering the best overall performance.

6.3 Sampling Steps

We also investigate the quality of TESS generations on the suite of NLG tasks as well as MRPC by varying the number of sampling steps during inference. Slow sampling speed is a major obstacle for most current text diffusion models, and prior work, e.g., [Li et al. \(2022b\)](#), suffers from a significant drop in generation quality when reducing

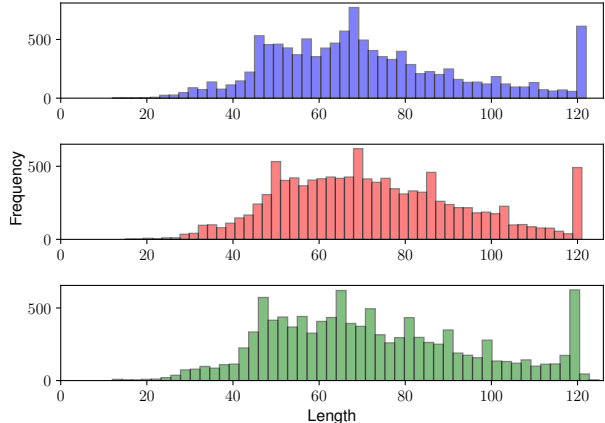


Figure 2: From top to bottom: (a) distribution of target lengths; (b) distribution of predicted length by BART; (c) distribution of predicted length by TESS.

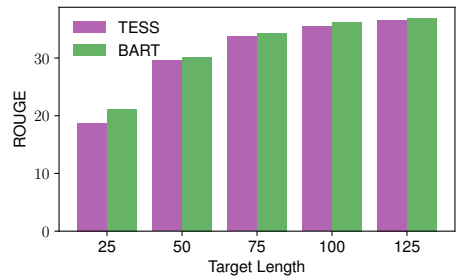


Figure 3: Average ROUGE score (R1, R2, R-L) for our model and BART for variable target length. Our method performs comparably to BART for different target lengths.

the number of sampling steps. As shown in Table 7, TESS performs well with relatively few steps, with only a marginal drop in performance even when sampling steps are decreased from 1000 to 100. For classification tasks that involve shorter generation (MRPC), 10 sampling steps result in lossless quality. However, for tasks that require longer generation such as summarization, 10 steps substantially reduce performance, as expected.

6.4 Sampling Speed

As shown in Section §5, TESS consistently outperforms SSD-LM under an equivalent setup. We continue this comparison by considering the time it takes to sample from each model. Compared to SSD-LM, which decodes semi-autoregressively in blocks, TESS uses fully non-autoregressive decoding, which can provide substantial speed-ups over SSD-LM for long sequences. Consider the cost of generating T tokens with D diffusion steps and a

Method	MNLI	QNLI	QQP	RTE	SST-2	MRPC	CoLA	STS-B	WNLI	Average
RoBERTa _{large}	90.2/90.2	94.7	92.2	86.6	96.4	90.9	68.0	92.4	91.3	88.9
TESS _{large} (Ours)	90.1/89.8	94.2	89.1	88.5	96.4	93.1	67.7	88.9	83.1	88.5

Table 5: Comparison of TESS and RoBERTa on GLUE tasks on the development set.⁸ Following Devlin et al. (2019), we report F1 scores for MRPC and QQP; STS-B, Spearman correlation coefficient; CoLA, Matthews correlation; all other tasks, accuracy. Bold fonts indicate the best results. Following RoBERTa, both results on the development set are a median over five runs. Following RoBERTa for RTE, STS, and MRPC, we finetune starting from the MNLI model instead of the baseline pretrained model.

Model	TEXT SIMPLIFICATION			
	SARI	BLEU	BERT	R-L
TESS	44.1	30.8	78.8	52.6
+orig. self-cond	52.2	43.3	81.9	58.9
+proposed self-cond	54.2	40.8	82.0	59.3
PARAPHRASE GENERATION				
	BLEU	BERT	R-L	D-1/D-4
TESS	25.9	84.4	59.7	98.7/60.4
+orig. self-cond	28.4	85.5	61.7	98.6/60.6
+proposed self-cond	29.2	85.5	61.2	98.5/ 61.4

Table 6: Ablation on the effects of self-conditioning. We compare our proposed self-conditioning to the original method in Chen et al. (2022), and the model without self-conditioning. Bold fonts indicate the best results.

block size of B for SSD-LM. Since SSD-LM and TESS both use RoBERTa as their denoising backbones, running D diffusion steps takes $O(DT^2)$, including attention cost. Then SSD-LM decoding takes $O(\lceil T/B \rceil DT^2)$ time, as generating each block requires D diffusion steps, with the last block requiring attention over all T tokens. In contrast, TESS decoding takes $O(DT^2)$, as it generates all tokens in one pass. We also note that TESS works well with a far smaller D than SSD-LM, which uses at minimum 1000 diffusion steps. In contrast, TESS achieves strong performance with as few as 100 steps, as seen in Table 7.

We compare TESS generation times with other models in Figure 4. We time how long decoding 25 to 5000 tokens takes given a context of 50 tokens and 100 diffusion steps. We find that TESS is faster during inference than SSD-LM, especially when SSD-LM has to generate multiple blocks due to its limited block size. Notably, we find TESS is faster, albeit marginally, than an equivalently-sized BART when generating more than 2000 tokens. We provide further details on these experiments in Appendix A.3.

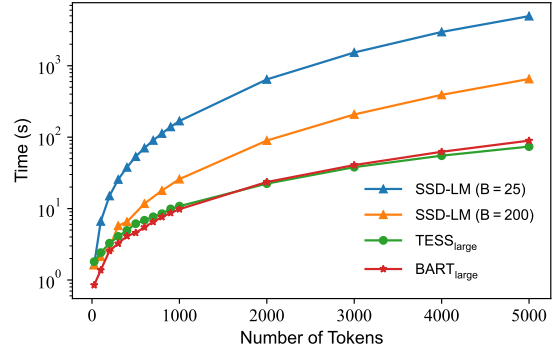


Figure 4: Time taken to generate the given number of tokens with 100 diffusion steps. We report the average time over five runs. Diffusion-based models use RoBERTa_{large} as their backbone.

7 Related Work

Diffusion for Continuous Domains Diffusion models were first proposed by Sohl-Dickstein et al. (2015), who approached generative modeling from a non-equilibrium thermodynamics point of view. In Denoising Diffusion Probabilistic Models (DDPMs), Ho et al. (2020) proposed a new parameterization that revealed an equivalence between ground-truth prediction and noise estimation. Song et al. (2021) proposed an alternative stochastic differential equation interpretation of diffusion that involves the Stein score function.

Nichol and Dhariwal (2021) proposed modifications to DDPMs, such as an improved cosine noise schedule and an importance-weighted loss objective, which improved log-likelihood and reduced the number of sampling steps. Ho and Salimans (2021) proposed classifier-free guidance, a technique that allows for highly controllable generation without the need for an external classifier to guide the score estimates of the generative model.

Continuous Diffusion for Discrete Domains Following the success of diffusion models on continuous domains, there have been several attempts

Steps	QQP	NEWSELA-AUTO	QG	CNN-DM	MRPC	
	R-L					Accuracy
10	62.4	58.4	38.8	35.6	89.7	92.8
100	62.0	59.1	38.9	39.6	89.7	92.8
1000	62.2	59.4	38.9	39.7	89.7	92.8

Table 7: Impact of number of sampling steps on performance. Our method achieves competitive results with as few as 10 or 100 steps on NLG tasks and 10 for MRPC.

to apply diffusion on discrete data. Li et al. (2022a) applied diffusion on the latent token embedding space. Their resulting language model relies on word-level tokenization and works mostly on small-scale datasets with a short sequence length of 64 tokens. They also investigated controlled sequence generation by leveraging additional syntactic and semantic information, with little focus on evaluation for cases when additional syntactic information did not exist. Li et al. (2022a) trained the model to predict the noise added to the embeddings with a regression loss, which can have a trivial solution if all embeddings represent the same vector (Dieleman et al., 2022). Therefore, an additional loss term was added to the training objective, and controlled generation is necessary to avoid the collapse (Li et al., 2022a).

Strudel et al. (2022) used frozen pretrained word embedding with careful scaling to address the instability resulting from the competition between diffusion and reconstruction loss. However, their method does not allow the joint training of word embeddings and the diffusion model. The resulting model was also not evaluated on actual downstream NLP tasks. More recently, Dieleman et al. (2022) attempted to learn the embedding and diffusion model jointly, still by performing diffusion in the embedding space. Other recent works have also applied diffusion on word embeddings to tackle sequence-to-sequence problems (Gong et al., 2022; Yuan et al., 2022). Concurrent to our work, Ye et al. (2023) further analyzed the approach of Li et al. (2022b) and proposed methods for manipulating the noise in the diffusion process during training and inference, yielding improved conditional text generation.

Recently, Han et al. (2022) proposed a semi-autoregressive diffusion model which generates small blocks of 25 tokens from left to right while allowing bidirectional context within the blocks. Deviating from prior work, their approach is based on simplex diffusion (Richemond et al., 2022), i.e.,

the diffusion process occurs in the vocabulary logit space rather than the typical embedding space. We follow this formulation but extend their approach to fully non-autoregressive generation and incorporate an efficient self-conditioning method that exploits the semantics of the simplex space.

Discrete Diffusion for Discrete Domains Unlike continuous diffusion models, discrete diffusion models maintain the discrete structure of the data domain and perform state transitions based on a probability matrix. Diffusion models with discrete state space were first explored by Sohl-Dickstein et al. (2015), who proposed a framework for diffusion over binary random variables. Later, Hoogeboom et al. (2021) and Austin et al. (2021) proposed discrete diffusion models for categorical random variables. However, these methods generally lag behind autoregressive models. More recently, Reid et al. (2022) proposed Diffuser, which formulates a discrete diffusion process by modeling text generation as a series of discrete edit operations.

8 Conclusion

We present TESS, a new sequence-to-sequence diffusion model for language generation tasks that is fully non-autoregressive, works for longer sequences, performs the diffusion process on the vocabulary logit space, and employs a new and efficient form of self-conditioning. TESS outperforms strong autoregressive baselines as well as recent state-of-the-art text diffusion models on a wide variety of conditional language generation and language understanding tasks. Experimental results show that simplex diffusion substantially outperforms other diffusion methods that involve the hidden embedding space. Future work relies on pretraining our method combined with denoising and infilling objectives, e.g., Bavarian et al. (2022), which we hypothesize can provide further performance boosts to our text-to-text diffusion model.

Limitations

Sampling Speed It is well-known that generating samples from a diffusion model is slow due to the iterative nature of the sampling process. In this work, we experiment with varying levels of sampling steps to demonstrate that TESS performs competitively without performing the full backward process. We hypothesize that this is due to the discrete nature of the logit simplex and the use of the argmax operator, which acts as a corrector that projects noisy predictions back into the k -logit simplex. Given ongoing developments in adjacent fields to accelerate sampling in diffusion-based models (Song et al., 2023), we expect further performance gains by leveraging the unique characteristics of the logit simplex.

Long Sequence Inference speed tests with SSD-LM and BART show that TESS quickly dominates semi-autoregressive generation and outperforms BART at 2000 tokens. This result suggests that diffusion models have the potential of being faster than popular autoregressive models at long sequence lengths. In this work, we primarily used RoBERTa_{base} models to facilitate fair comparison with existing baselines, which inevitably limited the size of the context window due to the absolute position embedding strategy employed by RoBERTa. We suspect that unlocking the full potential of diffusion-based language models may lie in the long sequence regime, which could involve scaling current models up to a larger size.

Acknowledgements

We are grateful to Aman Madaan, Robin Strudel, Sander Dieleman, Chris Dyer, Xiaochuang Han, Sachin Kumar, Clara Meister, Sean Welleck, and Andre Wibisono for helpful comments and discussions, and Sam Skjonsberg and the ReViz team at AI2 for their support in managing experiments.

References

Jacob Austin, Daniel D. Johnson, Jonathan Ho, Daniel Tarlow, and Rianne van den Berg. 2021. Structured denoising diffusion models in discrete state-spaces. In *NeurIPS*.

Roy Bar-Haim, Ido Dagan, Bill Dolan, Lisa Ferro, and Danilo Giampiccolo. 2006. The second pascal recognising textual entailment challenge. *Second PASCAL Challenges Workshop on Recognising Textual Entailment*.

Mohammad Bavarian, Heewoo Jun, Nikolas A. Tezak, John Schulman, Christine McLeavey, Jerry Tworek, and Mark Chen. 2022. Efficient training of language models to fill in the middle. *ArXiv*, abs/2207.14255.

Luisa Bentivogli, Ido Dagan, Hoa Trang Dang, Danilo Giampiccolo, and Bernardo Magnini. 2009. The fifth pascal recognizing textual entailment challenge. In *TAC*.

Daniel Cer, Mona Diab, Eneko Agirre, Iñigo Lopez-Gazpio, and Lucia Specia. 2017. *SemEval-2017 task 1: Semantic textual similarity multilingual and crosslingual focused evaluation*. In *Proceedings of the 11th International Workshop on Semantic Evaluation (SemEval-2017)*, pages 1–14, Vancouver, Canada. Association for Computational Linguistics.

Ting Chen, Ruixiang Zhang, and Geoffrey Hinton. 2022. Analog bits: Generating discrete data using diffusion models with self-conditioning. *arXiv preprint arXiv:2208.04202*.

Ido Dagan, Oren Glickman, and Bernardo Magnini. 2005. The pascal recognising textual entailment challenge. In *Machine Learning Challenges Workshop*.

Aditya Deshpande, Jyoti Aneja, Liwei Wang, Alexander G. Schwing, and David A. Forsyth. 2018. Fast, diverse and accurate image captioning guided by part-of-speech. *2019 IEEE/CVF Conference on Computer Vision and Pattern Recognition (CVPR)*, pages 10687–10696.

Jacob Devlin, Ming-Wei Chang, Kenton Lee, and Kristina Toutanova. 2019. *BERT: Pre-training of deep bidirectional transformers for language understanding*. In *Proceedings of the 2019 Conference of the North American Chapter of the Association for Computational Linguistics: Human Language Technologies, Volume 1 (Long and Short Papers)*, pages 4171–4186, Minneapolis, Minnesota. Association for Computational Linguistics.

Bhuwan Dhingra, Kathryn Mazaitis, and William W Cohen. 2017. Quasar: Datasets for question answering by search and reading. *arXiv preprint arXiv:1707.03904*.

Sander Dieleman, Laurent Sartran, Arman Roshan-nai, Nikolay Savinov, Yaroslav Ganin, Pierre H Richemond, Arnaud Doucet, Robin Strudel, Chris Dyer, Conor Durkan, et al. 2022. Continuous diffusion for categorical data. *arXiv preprint arXiv:2211.15089*.

William B. Dolan and Chris Brockett. 2005. *Automatically constructing a corpus of sentential paraphrases*. In *Proceedings of the Third International Workshop on Paraphrasing (IWP2005)*.

Wanyu Du, Jianqiao Zhao, Liwei Wang, and Yangfeng Ji. 2022. Diverse text generation via variational encoder-decoder models with gaussian process priors. *arXiv preprint arXiv:2204.01227*.

Danilo Giampiccolo, Bernardo Magnini, Ido Dagan, and Bill Dolan. 2007. *The third PASCAL recognizing textual entailment challenge*. In *Proceedings of the ACL-PASCAL Workshop on Textual Entailment and Paraphrasing*, pages 1–9, Prague. Association for Computational Linguistics.

Shansan Gong, Mukai Li, Jiangtao Feng, Zhiyong Wu, and LingPeng Kong. 2022. Diffuseq: Sequence to sequence text generation with diffusion models. *arXiv preprint arXiv:2210.08933*.

Jiatao Gu, Changhan Wang, and Junbo Zhao. 2019. Levenshtein transformer. *NeurIPS*.

Xiaochuang Han, Sachin Kumar, and Yulia Tsvetkov. 2022. Ssd-lm: Semi-autoregressive simplex-based diffusion language model for text generation and modular control. *arXiv preprint arXiv:2210.17432*.

Karl Moritz Hermann, Tomas Kociský, Edward Grefenstette, Lasse Espeholt, Will Kay, Mustafa Suleyman, and Phil Blunsom. 2015. Teaching machines to read and comprehend. In *NeurIPS*.

Jonathan Ho, Ajay Jain, and Pieter Abbeel. 2020. Denoising diffusion probabilistic models. *NeurIPS*.

Jonathan Ho and Tim Salimans. 2021. Classifier-free diffusion guidance. In *NeurIPS Workshop DGMs Applications*.

Jonathan Ho, Tim Salimans, Alexey A Gritsenko, William Chan, Mohammad Norouzi, and David J Fleet. 2022. Video diffusion models. In *ICLR Workshop on Deep Generative Models for Highly Structured Data*.

Emiel Hoogeboom, Didrik Nielsen, Priyank Jaini, Patrick Forré, and Max Welling. 2021. Argmax flows and multinomial diffusion: Learning categorical distributions. *NeurIPS*.

Chao Jiang, Mounica Maddela, Wuwei Lan, Yang Zhong, and Wei Xu. 2020. Neural crf model for sentence alignment in text simplification. In *ACL*.

Zhifeng Kong, Wei Ping, Jiaji Huang, Kexin Zhao, and Bryan Catanzaro. 2020. Diffwave: A versatile diffusion model for audio synthesis. In *ICLR*.

Mike Lewis, Yinhan Liu, Naman Goyal, Marjan Ghazvininejad, Abdelrahman Mohamed, Omer Levy, Veselin Stoyanov, and Luke Zettlemoyer. 2020. Bart: Denoising sequence-to-sequence pre-training for natural language generation, translation, and comprehension. In *ACL*.

Quentin Lhoest, Albert Villanova del Moral, Yacine Jernite, Abhishek Thakur, Patrick von Platen, Suraj Patil, Julien Chaumond, Mariama Drame, Julien Plu, Lewis Tunstall, Joe Davison, Mario Šaško, Gunjan Chhablani, Bhavitvyा Malik, Simon Brandeis, Teven Le Scao, Victor Sanh, Canwen Xu, Nicolas Patry, Angelina McMillan-Major, Philipp Schmid, Sylvain Gugger, Clément Delangue, Théo Matussière, Lysandre Debut, Stas Bekman, Pierrick Cistac, Thibault Goehringer, Victor Mustar, François Lagunas, Alexander Rush, and Thomas Wolf. 2021. *Datasets: A community library for natural language processing*. In *Proceedings of the 2021 Conference on Empirical Methods in Natural Language Processing: System Demonstrations*, pages 175–184, Online and Punta Cana, Dominican Republic. Association for Computational Linguistics.

Xiang Lisa Li, John Thickstun, Ishaan Gulrajani, Percy Liang, and Tatsunori Hashimoto. 2022a. Diffusion-LM improves controllable text generation. In *NeurIPS*.

Xiang Lisa Li, John Thickstun, Ishaan Gulrajani, Percy Liang, and Tatsunori B Hashimoto. 2022b. Diffusion-lm improves controllable text generation. In *NeurIPS*.

Chin-Yew Lin. 2004. *ROUGE: A package for automatic evaluation of summaries*. In *Text Summarization Branches Out*, pages 74–81, Barcelona, Spain. Association for Computational Linguistics.

Yinhan Liu, Myle Ott, Naman Goyal, Jingfei Du, Mandar Joshi, Danqi Chen, Omer Levy, Mike Lewis, Luke Zettlemoyer, and Veselin Stoyanov. 2019. *Roberta: A robustly optimized BERT pretraining approach*. *CoRR*, abs/1907.11692.

Alexander Quinn Nichol and Prafulla Dhariwal. 2021. Improved denoising diffusion probabilistic models. In *ICML*.

Kishore Papineni, Salim Roukos, Todd Ward, and Wei-Jing Zhu. 2002. *Bleu: a method for automatic evaluation of machine translation*. In *Proceedings of the 40th Annual Meeting of the Association for Computational Linguistics*, pages 311–318, Philadelphia, Pennsylvania, USA. Association for Computational Linguistics.

Alec Radford, Jeffrey Wu, Rewon Child, David Luan, Dario Amodei, Ilya Sutskever, et al. 2019. Language models are unsupervised multitask learners. *OpenAI blog*.

Colin Raffel, Noam Shazeer, Adam Roberts, Katherine Lee, Sharan Narang, Michael Matena, Yanqi Zhou, Wei Li, and Peter J Liu. 2020. Exploring the limits of transfer learning with a unified text-to-text transformer. *JMLR*.

Pranav Rajpurkar, Jian Zhang, Konstantin Lopyrev, and Percy Liang. 2016. *SQuAD: 100,000+ questions for machine comprehension of text*. In *Proceedings of the 2016 Conference on Empirical Methods in Natural Language Processing*, pages 2383–2392, Austin, Texas. Association for Computational Linguistics.

Aditya Ramesh, Prafulla Dhariwal, Alex Nichol, Casey Chu, and Mark Chen. 2022. Hierarchical text-conditional image generation with clip latents. *arXiv preprint arXiv:2204.06125*.

Machel Reid, Vincent J Hellendoorn, and Graham Neubig. 2022. Diffuser: Discrete diffusion via edit-based reconstruction. *arXiv preprint arXiv:2210.16886*.

Pierre H Richemond, Sander Dieleman, and Arnaud Doucet. 2022. Categorical sdes with simplex diffusion. *arXiv preprint arXiv:2210.14784*.

Chitwan Saharia, William Chan, Saurabh Saxena, Lala Li, Jay Whang, Emily Denton, Seyed Kamyar Seyed Ghasemipour, Burcu Karagol Ayan, S Sara Mahdavi, Rapha Gontijo Lopes, et al. 2022. Photorealistic text-to-image diffusion models with deep language understanding. In *NeurIPS*.

Nikolay Savinov, Junyoung Chung, Mikolaj Binkowski, Erich Elsen, and Aaron van den Oord. 2021. Step-unrolled denoising autoencoders for text generation. In *ICLR*.

Kai Shen, Zeqian Ju, Xu Tan, Yanqing Liu, Yichong Leng, Lei He, Tao Qin, Sheng Zhao, and Jiang Bian. 2023. Naturalspeech 2: Latent diffusion models are natural and zero-shot speech and singing synthesizers. *ArXiv*, abs/2304.09116.

Richard Socher, Alex Perelygin, Jean Wu, Jason Chuang, Christopher D. Manning, Andrew Ng, and Christopher Potts. 2013. Recursive deep models for semantic compositionality over a sentiment treebank. In *Proceedings of the 2013 Conference on Empirical Methods in Natural Language Processing*, pages 1631–1642, Seattle, Washington, USA. Association for Computational Linguistics.

Jascha Sohl-Dickstein, Eric Weiss, Niru Maheswaranathan, and Surya Ganguli. 2015. Deep unsupervised learning using nonequilibrium thermodynamics. In *ICML*.

Jiaming Song, Chenlin Meng, and Stefano Ermon. 2020. Denoising diffusion implicit models. In *ICLR*.

Yang Song, Prafulla Dhariwal, Mark Chen, and Ilya Sutskever. 2023. Consistency models. In *ICML*.

Yang Song, Jascha Sohl-Dickstein, Diederik P. Kingma, Abhishek Kumar, Stefano Ermon, and Ben Poole. 2021. Score-based generative modeling through stochastic differential equations. In *ICLR*.

Robin Strudel, Corentin Tallec, Florent Altché, Yilun Du, Yaroslav Ganin, Arthur Mensch, Will Grathwohl, Nikolay Savinov, Sander Dieleman, Laurent Sifre, et al. 2022. Self-conditioned embedding diffusion for text generation. *arXiv preprint arXiv:2211.04236*.

Ashish Vaswani, Noam Shazeer, Niki Parmar, Jakob Uszkoreit, Llion Jones, Aidan N Gomez, Łukasz Kaiser, and Illia Polosukhin. 2017. Attention is all you need. *NeurIPS*.

Alex Wang, Amanpreet Singh, Julian Michael, Felix Hill, Omer Levy, and Samuel R. Bowman. 2019. GLUE: A multi-task benchmark and analysis platform for natural language understanding. In *ICLR*.

Alex Warstadt, Amanpreet Singh, and Samuel R. Bowman. 2019. Neural network acceptability judgments. *Transactions of the Association for Computational Linguistics*, 7:625–641.

Adina Williams, Nikita Nangia, and Samuel Bowman. 2018. A broad-coverage challenge corpus for sentence understanding through inference. In *Proceedings of the 2018 Conference of the North American Chapter of the Association for Computational Linguistics: Human Language Technologies, Volume 1 (Long Papers)*, pages 1112–1122, New Orleans, Louisiana. Association for Computational Linguistics.

Thomas Wolf, Lysandre Debut, Victor Sanh, Julien Chaumond, Clement Delangue, Anthony Moi, Pierrette Cistac, Tim Rault, Rémi Louf, Morgan Funtowicz, Joe Davison, Sam Shleifer, Patrick von Platen, Clara Ma, Yacine Jernite, Julien Plu, Canwen Xu, Teven Le Scao, Sylvain Gugger, Mariama Drame, Quentin Lhoest, and Alexander M. Rush. 2020. Transformers: State-of-the-art natural language processing. In *EMNLP: System Demonstrations*.

Wei Xu, Chris Callison-Burch, and Courtney Napoles. 2015. Problems in current text simplification research: New data can help. *Transactions of the Association for Computational Linguistics*, 3:283–297.

Wei Xu, Courtney Napoles, Ellie Pavlick, Quanze Chen, and Chris Callison-Burch. 2016. Optimizing statistical machine translation for text simplification. *TACL*.

Jiasheng Ye, Zaixiang Zheng, Yu Bao, Lihua Qian, and Mingxuan Wang. 2023. Dinoiser: Diffused conditional sequence learning by manipulating noises.

Hongyi Yuan, Zheng Yuan, Chuanqi Tan, Fei Huang, and Songfang Huang. 2022. Seqdiffuseq: Text diffusion with encoder-decoder transformers. *arXiv preprint arXiv:2212.10325*.

Tianyi Zhang, Varsha Kishore, Felix Wu, Kilian Q Weinberger, and Yoav Artzi. 2020. BERTscore: Evaluating text generation with BERT. In *ICLR*.

A Experiment Details

A.1 Dataset

NEWSLEA-AUTO dataset (Jiang et al., 2020) is based on a Xu et al. (2015) with revised alignment and improved quantity and quality. For question generation, we use the QUASAR-T dataset (Dhingra et al., 2017); for summarization, CNN-DailyMail (Hermann et al., 2015).

The GLUE benchmark (Wang et al., 2019) is released under the Creative Commons License (CC BY 4.0). This benchmark consists of multiple datasets: SST-2 (Socher et al., 2013), MNLI (Williams et al., 2018), CoLA (Warstadt et al., 2019), MRPC (Dolan and Brockett, 2005), QQP⁹, QNLI (Rajpurkar et al., 2016), STS-B (Cer et al., 2017), and RTE, which is a combination of data from RTE1 (Dagan et al., 2005), RTE2 (Bar-Haim et al., 2006), RTE3 (Giampiccolo et al., 2007), RTE5 (Bentivogli et al., 2009). We download all datasets from the Hugging Face Datasets library (Lhoest et al., 2021). Table 8 shows the sequence lengths for the source and target in each dataset, in number of tokens.

Dataset	Source	Target
GLUE	128	5
NEWSLEA-AUTO	128	128
QQP	100	85
QG	155	65
CNN-DM	392	120

Table 8: Sequence length of each dataset.

A.2 Training Hyperparameters

We trained our models with a learning rate of $3e-5$ with the AdamW optimizer, with default parameters $\beta_1 = 0.9$, $\beta_2 = 0.999$, $\epsilon = 1e-8$. For self-conditioning in Equation (11), we set $\rho = 0.5$ during training; during inference, we always apply self-conditioning ($\rho = 1$).

For the experiments on GLUE, we set the number of warm-up steps to 500 with a default linear learning rate scheduler. We trained the larger datasets in GLUE for 25K steps; for smaller datasets, 12K steps. We then evaluate the models every 1K steps and report the results on the checkpoint obtaining the best results on the development set.

For all generation tasks, we train our method and BART for paraphrase generation, summarization, question generation, and text simplification for 90K, 120K, 120K, and 80K steps, respectively. We set the number of warmup steps to 2000 for all generation tasks.

A.3 Inference Speed Experiments

For the inference speed numbers reported in Table 4, we run all experiments on a single 80 GB NVIDIA A100 GPU. We use an adapted version of the SSD-LM inference script provided by the authors in their public repository, removing unnecessary logging and slowdowns. For BART_{large}, we use the transformers library (Wolf et al., 2020). We alter all models to allow sequence lengths over 512 tokens by resizing the position embeddings matrix. We use the following context: *“A man of innumerable personalities and powers vs. the most powerful artificial intelligence in this universe: Legion vs. Nimrod! With Nightcrawler in Orchis clutches, David Haller and his allies will have to confront the mastermind who”*. We report the exact timings and standard deviations in Table 9.

B Inference Step

Although we employ the same sampling procedure as Han et al. (2022), their derivation requires specific assumptions on the noise schedule. Specifically, they assume a cosine noise schedule (Nichol and Dhariwal, 2021), where $\sqrt{(\alpha_t - \bar{\alpha}_t)/(1 - \bar{\alpha}_t)} \geq 0.98$ for 98% of $t \in \{1, 2, \dots, T\}$, with some outliers at the boundaries. Here, we outline an alternate derivation based on DDIM (Song et al., 2020), which yields the same sampling procedure as SSD-LM without being restricted to a particular noise schedule.

Song et al. (2020) generalized DDPMs (Ho et al., 2020) by constructing a non-Markovian forward process. Despite this difference, DDIMs and DDPMs remarkably share the same training objective; hence, a trained DDPM model can also be used as a DDIM without modification or additional training simply by following a different sampling procedure. The DDIM reverse process can be written as

$$q_\sigma(\mathbf{x}_{t-1} | \mathbf{x}_t, \mathbf{x}_0) = \mathcal{N}(\boldsymbol{\mu}_{t-1}, \sigma_t^2 \mathbf{I}),$$

where the mean $\boldsymbol{\mu}_{t-1}$ is given by

$$\sqrt{\alpha_{t-1}} \mathbf{x}_0 + \sqrt{1 - \alpha_{t-1} - \sigma_t^2} \cdot \frac{\mathbf{x}_t - \sqrt{\alpha_t} \mathbf{x}_0}{\sqrt{1 - \alpha_t}}.$$

⁹<https://quoradata.quora.com/First-Quora-Dataset-Release-Question-Pairs>

Model	Blocks	Number of Tokens														
		25	100	200	300	400	500	600	700	800	900	1000	2000	3000	4000	5000
SSD-LM	25	1.6 _{0.3}	6.6 _{0.3}	15.0 _{0.3}	25.6 _{0.3}	37.8 _{0.3}	53.4 _{0.4}	70.4 _{0.0}	90.1 _{0.0}	112.7 _{0.0}	139.4 _{0.0}	168.4 _{0.0}	643.2 _{0.2}	1531.5 _{0.6}	2933.4 _{0.9}	4945.1 _{2.7}
SSD-LM	200	1.6 _{0.3}	2.1 _{0.3}	2.8 _{0.3}	5.8 _{0.3}	6.5 _{0.3}	-	11.7 _{0.3}	-	17.9 _{0.0}	-	25.8 _{0.0}	89.6 _{0.0}	207.8 _{0.0}	391.1 _{0.2}	652.2 _{0.2}
BART _{large}	-	0.8 _{0.2}	1.4 _{0.2}	2.6 _{0.2}	3.2 _{0.2}	4.1 _{0.2}	4.6 _{0.2}	5.5 _{0.0}	6.5 _{0.0}	7.6 _{0.0}	8.7 _{0.0}	9.8 _{0.0}	23.5 _{0.2}	40.6 _{0.1}	62.4 _{0.1}	89.4 _{0.4}
TESS-100	-	1.8 _{0.3}	2.4 _{0.3}	3.3 _{0.3}	4.1 _{0.3}	4.9 _{0.3}	6.1 _{0.3}	6.9 _{0.0}	7.7 _{0.0}	8.5 _{0.0}	9.9 _{0.0}	10.8 _{0.0}	22.3 _{0.0}	38.0 _{0.0}	55.0 _{0.0}	73.8 _{0.0}

Table 9: Time taken to generate the given number of tokens with a 50-token prefix. SSD-LM and TESS-100 use 100 diffusion steps and a RoBERTa_{large} underlying model. All values are the average over 5 runs, with standard deviations given as subscripts (note that many standard deviations were less than 0.05, and so appear as 0.0).

Notably, setting $\sigma_t = 0$ for all $t \in \{1, 2, \dots, T\}$ and using the model prediction $\hat{\mathbf{x}}_0$ instead of the ground truth \mathbf{x}_0 yield a deterministic sampling process

$$\begin{aligned}\mathbf{x}_{t-1} &= \sqrt{\alpha_{t-1}} \hat{\mathbf{x}}_0 + \sqrt{1 - \alpha_{t-1}} \cdot \frac{\mathbf{x}_t - \sqrt{\alpha_t} \hat{\mathbf{x}}_0}{\sqrt{1 - \alpha_t}} \\ &= \sqrt{\alpha_{t-1}} \hat{\mathbf{x}}_0 + \sqrt{1 - \alpha_{t-1}} \hat{\boldsymbol{\epsilon}}_t,\end{aligned}$$

where the last equality follows from a simple reparametrization of the forward process in Equation (2), i.e.,

$$\begin{aligned}\mathbf{x}_t &= \sqrt{\alpha_t} \mathbf{x}_0 + \sqrt{1 - \alpha_t} \boldsymbol{\epsilon}_t \\ \iff \hat{\boldsymbol{\epsilon}}_t &= \frac{\mathbf{x}_t - \sqrt{\alpha_t} \hat{\mathbf{x}}_0}{\sqrt{1 - \alpha_t}}.\end{aligned}$$

Replacing \mathbf{x} with \mathbf{S} for change in notation recovers the sampling process in Equation (9). Concretely, we can use Equation (10) to project the prediction into the k -logit simplex, producing $\hat{\mathbf{S}}_0$, which is in turn used to compute $\hat{\boldsymbol{\epsilon}}_t$.

Although the derivation in Han et al. (2022) also leads to a deterministic sampling procedure, in practice, they sample $\boldsymbol{\epsilon}$ from the noise prior $\mathcal{N}(0, k^2 \mathbf{I})$. Empirically, we found that deterministic sampling and stochastic sampling yielded similar results, with the former being marginally worse in some cases. Moreover, since TESS and SSD-LM are both trained on a modified objective that involves cross-entropy loss instead of the standard mean squared error, we hypothesize that there could be divergent behavior during sampling that requires a more principled investigation. We leave this as a subject for future study.

C Qualitative Examples

We show non-cherry-picked example outputs from TESS model and BART, the strongest baseline, on the summarization task in Table 10. Qualitatively, we observe that TESS is capable of generating natural samples that are often indistinguishable from those of BART.

Gold	BART	Ours
Membership gives the ICC jurisdiction over alleged crimes committed in Palestinian territories since last June. Israel and the United States opposed the move, which could open the door to war crimes investigations against Israelis.	The Palestinian Authority officially becomes the 123rd member of the International Criminal Court. It gives the court jurisdiction over alleged crimes committed in Palestinian territories. Israel and the United States, neither of which is an ICC member, opposed the Palestinians' efforts to join the body.	The Palestinian Authority is the 123rd member of the International Criminal Court. The move gives it jurisdiction over alleged crimes in Palestinian territories. Israel and the United States oppose the Palestinians' efforts to join it.
Theia, a bully breed mix, was apparently hit by a car, whacked with a hammer and buried in a field. "She's a true miracle dog and she deserves a good life," says Sara Mellado, who is looking for a home for Theia.	A stray pooch in Washington State has used up at least three of her own injuries. Theia, a bully breed mix, was hit by a car and then buried in a field. She has been receiving care at the Veterinary Teaching Hospital.	A stray dog was found on a farm in Washington State. The dog has used up at least three of her own after being hit in the head by a car and being buried in a field. Theia has a dislocated jaw, leg injuries and needs surgery to help breathe.
Mohammad Javad Zarif has spent more time with John Kerry than any other foreign minister. He once participated in a takeover of the Iranian Consulate in San Francisco. The Iranian foreign minister tweets in English.	Mohammad Javad Zarif is the Iranian foreign minister. He has been John Kerry's opposite number in securing a breakthrough in nuclear talks.	Mohammad Javad Zarif is now Iran's foreign minister. He has been John Kerry's opposite number in securing a breakthrough in nuclear talks.
17 Americans were exposed to the Ebola virus while in Sierra Leone in March. Another person was diagnosed with the disease and taken to hospital in Maryland. National Institutes of Health says the patient is in fair condition after weeks of treatment.	One of the five had a heart-related issue on Saturday and has been discharged. The others have already gone home.	Five Americans were monitored for three weeks at an Omaha hospital. One of the five had a heart-related issue on Saturday. The others have already gone home. They were exposed to Ebola in Sierra Leone, but none developed the deadly virus.
Student is no longer on Duke University campus and will face disciplinary review. School officials identified student during investigation and the person admitted to hanging the noose, Duke says. The noose, made of rope, was discovered on campus about 2 a.m.	A student admitted to hanging a noose made of rope from a tree near a student union. Duke didn't identify the student, citing federal privacy laws. The incident is one of several recent racist events to affect college students.	A Duke student admitted to hanging a noose from a tree. The private school didn't identify the student, citing federal privacy laws. The student is no longer on campus and will face student conduct review.
College-bound basketball star asks girl with Down syndrome to high school prom. Pictures of the two during the "prom-posal" have gone viral.	Eastern High School basketball player Trey Moses asked his girlfriend to be his prom date. Ellie Meredith, a freshman with Down syndrome, has struggled with friendships since elementary school. A special program at Eastern has made things easier for her, her mom says.	College basketball player and high school freshman picked Ellie Meredith as his prom date. The photos have gone viral on social media.
Amnesty's annual death penalty report catalogs encouraging signs, but setbacks in numbers of those sentenced to death. Organization claims that governments around the world are using the threat of terrorism to advance executions. The number of executions worldwide has gone down by almost 22% compared with 2013, but death sentences up by 28%.	Amnesty International says governments are using the death penalty to advance executions. At least 607 people were executed around the world in 2014, compared to 778 in 2013.	Amnesty International released its annual report on the death penalty. At least 607 people were executed in 2014, compared to 778 in 2013. Report cites Pakistan lifting a six-year moratorium on the execution of civilians. China has used the death penalty as a tool in its "Strike Hard" campaign against terrorism in the restive far-western province of Xinjiang.
Andrew Getty's death appears to be from natural causes, police say, citing coroner's early assessment. In a petition for a restraining order, Getty had written he had a serious medical condition. Police say this is not a criminal matter at this time.	Andrew Getty appears to have died of natural causes, police say. The coroner's preliminary assessment is there was no foul play involved in his death. He was the grandson of oil tycoon J. Paul Getty.	Coroner's preliminary assessment says there was no foul play involved in the death of Getty. Andrew Getty, 47, had "several health issues," detective says. There is no criminal investigation underway, detective says.
Once a super typhoon, Maysak is now a tropical storm with 70 mph winds. It could still cause flooding, landslides and other problems in the Philippines.	Maysak has lost a lot of steam as it spins west in the Pacific Ocean. It boasts steady winds of more than 70 mph (115 kph) and gusts up to 90 mph.	Maysak gained super typhoon status thanks to sustained 150 mph winds. Authorities have forbanned outdoor activities like swimming, surfing, diving and boating in some locales.

Table 10: Non-cherry-picked generated samples on the CNN-DM dataset from BART and TESS.